Pergamon

Bioorganic & Medicinal Chemistry Letters 11 (2001) 803–807

BIOORGANIC &
MEDICINAL
CHEMISTRY
LETTERS

Discovery of Zoniporide: A Potent and Selective Sodium–Hydrogen Exchanger Type 1 (NHE-1) Inhibitor with High Aqueous Solubility

Angel Guzman-Perez,* Ronald T. Wester, Mary C. Allen, Janice A. Brown, Allan R. Buchholz, Ewell R. Cook, Wesley W. Day, Ernest S. Hamanaka, Scott P. Kennedy, Delvin R. Knight, Paul J. Kowalczyk, Ravi B. Marala, Christian J. Mularski, William A. Novomisle, Roger B. Ruggeri, W. Ross Tracey and Roger J. Hill

Pfizer Global Research and Development, Pfizer Inc., Eastern Point Road, Groton CT 06340, USA

Received 20 October 2000; accepted 24 January 2001

Abstract—Zoniporide (CP-597,396) is a potent and selective inhibitor of NHE-1, which exhibits high aqueous solubility and acceptable pharmacokinetics for intravenous administration. The discovery, synthesis, activities, and rat and dog pharmacokinetics of this compound are presented. The potency and selectivity of zoniporide may be due to the conformation that the molecule adopts due to the presence of a cyclopropyl and a 5-quinolinyl substituent on the central pyrazole ring of the molecule. © 2001 Elsevier Science Ltd. All rights reserved.

The sodium–hydrogen exchangers (NHEs) are cell membrane transport proteins which exchange extracellular Na^+ for intracellular H^+ driven by concentration gradients. NHEs play a key role in intracellular pH regulation, ion-transport and control of cell volume. There are at least six known isoforms that are designated NHE-1 through NHE-6.[1] NHE-1 appears to play a key role in mediating myocardial injury during periods of ischemia and reperfusion. Although there is some debate about the degree of NHE-1 activity during myocardial ischemia, the activation of this exchanger during reperfusion is clearly detrimental to the heart, due to a cascade of increased intracellular Na^+, activation of the Na^+/Ca^{2+} exchanger, and intracellular Ca^{2+} overload. Consequently, inhibition of NHE-1, the sole isoform present in the heart, represents an attractive approach for reducing myocardial injury during ischemia/reperfusion.[2,3] A selective NHE-1 inhibitor is desirable due to the important physiological functions played by the additional NHE isoforms in other tissues. In particular, NHE-2 and NHE-3 appear to have significant roles in the gastrointestinal and renal systems.[1] The cardioprotective ability of a selective NHE-1 inhibitor could be extremely beneficial in hospital settings; for example, in patients that are at risk for myocardial ischemic injury during cardiac surgery.[2] For surgical settings, an agent with high aqueous solubility that would allow for intravenous administration would be preferred.

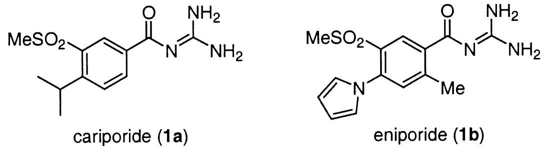

cariporide (**1a**) eniporide (**1b**)

Our efforts directed towards the discovery of a selective NHE-1 inhibitor began with the recognition that cariporide (**1a**)[4] and eniporide (**1b**),[5] two NHE inhibitors in clinical development, both contain an acylguanidine moiety. The synthesis and screening of a variety of heteroaryl acylguanidines led to the identification of pyrazole **3a** as a novel and attractive lead. Herein, we report the modifications in the structure of **3a** that led to the discovery of zoniporide (CP-597,396) (**3d**), a potent and selective NHE-1 inhibitor with the required aqueous solubility and pharmacokinetics for intravenous administration.

---

*Corresponding author. Tel.: +1-860-715-0313; fax: +1-860-686-0001; e-mail: angel_guzman-perez@groton.pfizer.com

0960-894X/01/$ - see front matter © 2001 Elsevier Science Ltd. All rights reserved.
PII: S0960-894X(01)00059-2

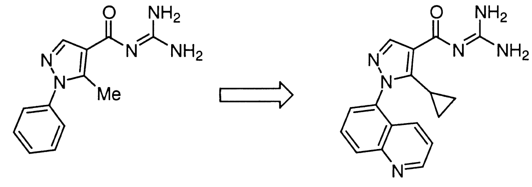

3a zoniporide (**3d**)

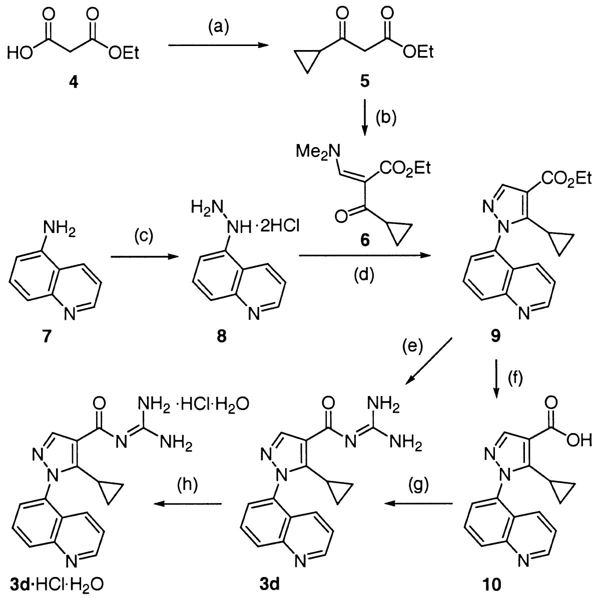

Scheme 1. Synthesis of zoniporide (**3d**) (a) (i) TMSCl, pyridine, ether, 23 °C, 4 h; (ii) *n*-BuLi (2.5 M in hexanes), −78 °C, 75 min; (iii) cyclopropanecarbonyl chloride, DME, −78–23 °C, 18 h, 93%; (b) *N*,*N*-dimethylformamide dimethyl acetal, reflux, 1 h, 91%; (c) (i) $NaNO_2$, H_2O, HCl (aq), 0 °C, 1 h; (ii) $SnCl_2{\cdot}2H_2O$, HCl (aq), 0–23 °C, 3 h; (iii) HCl (g), EtOAc, 0 °C, 15 min, 97%; (d) Et_3N, EtOH, reflux, 1 h, 88%; (e) guanidine, EtOH, 80 °C, in vacuo, 45 min, 76%; (f) NaOH (2 M aq), MeOH, reflux, 1 h, 56%; (g) (i) $SOCl_2$, reflux, 1 h; (ii) guanidine hydrochloride, NaOH (2 M aq), THF, reflux, 1 h, 67%; (h) HCl (conc), THF, 1 h, 82%.

The synthesis of **3d** is representative of that used to prepare similar analogues (Scheme 1). Monoethyl malonic ester (**4**) was converted to β-ketoester **5** by formation of the corresponding trimethylsilyl ester, followed by deprotonation with *n*-butyllithium and acylation with cyclopropanecarbonyl chloride.[6] Treatment of **5** with *N*,*N*-dimethylformamide dimethyl acetal provided enamine **6** as a single geometric isomer.[7] Hydrazine **8** was prepared by diazotization of amine **7** followed by reduction of the diazonium salt with stannous chloride and was isolated as the dihydrochloride salt.[8] This salt was considerably more stable to storage than the corresponding free base. The condensation of enamine **6** with hydrazine **8** in the presence of triethylamine afforded pyrazole ester **9** in good yield as the only detectable regioisomer.[7] This ester was converted to the acylguanidine by two different methods. In one method, a mixture of the ester and guanidine was heated first in ethanol, and then neat and in vacuo to provide **3d** as the free base. Alternatively, the ester was hydrolyzed to the corresponding carboxylic acid **10**, which was transformed to the acid chloride using thionyl chloride. The acid chloride was reacted with guanidine hydrochloride under Schotten–Baumann conditions to provide **3d** as the free base. In both cases, the free base **3d** was converted to the monohydrochloride salt which crystallized as the monohydrate **3d**·$HCl{\cdot}H_2O$.[9]

A fluorescence-imaging plate reader (FLIPR) assay was used as our primary screen for NHE-1 inhibitory activity. In this assay, fibroblasts expressing functional human NHE-1 were exposed to an intracellular acidic challenge in the presence of varying concentrations or absence of compound. The rate of NHE-1 mediated recovery of intracellular pH was determined in a 96-well format using the FLIPR and a pH sensitive fluorescent dye. NHE-1 inhibitors reduce the rate of pH recovery. The IC_{50} value is the concentration required to inhibit maximal pH recovery by 50%.[10] A similar assay with fibroblasts expressing human NHE-2 and rat NHE-3 was used to determine the inhibition of these isoforms.[10]

Table 1. NHE-1 and NHE-2 inhibitory activity and selectivity of zoniporide and analogues in vitro using a FLIPR based assay

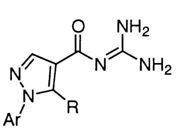

3

Compound[a]	R	Ar	NHE-1 IC_{50} (nM)[b]	NHE-2 IC_{50} (nM)[c]	NHE-1 versus NHE-2[d]
3a	Me	Ph	830	3900	5
3b	Cyclopropyl	Ph	350	12,800	37
3c	Cyclopropyl	1-Naphthyl	160	16,300	102
3d (Zoniporide)	Cyclopropyl	5-Quinolinyl	59	12,000	203
3e	Me	5-Quinolinyl	860	41,600	48
1a (Cariporide)	—	—	560	28,700	51
1b (Eniporide)	—	—	140	9200	66

[a] Experiments carried out using the hydrochloride or mesylate salt forms.
[b] Mean of 9–32 experiments.
[c] Mean of 6–13 experiments.
[d] NHE-1 versus NHE-2 selectivity (NHE-2 IC_{50}/NHE-1 IC_{50}).

As indicated in Table 1, the NHE-1 IC_{50} of lead compound **3a** is somewhat higher than that exhibited by reference compounds cariporide (**1a**) and eniporide (**1b**) in the FLIPR assay, and its NHE-1 versus NHE-2 selectivity is significantly lower. An investigation of the SAR around the methyl group of **3a** led to the identification of compound **3b** bearing a cyclopropyl group in its place. Compound **3b** has improved potency and considerably higher selectivity with respect to **3a**, and is comparable to cariporide and eniporide. Replacement of the phenyl ring with a 1-naphthyl ring provided compound **3c** with even greater potency and selectivity. Unfortunately, the moderate aqueous solubility of compound **3c** was not optimal for developing an intravenous formulation. To overcome this problem, the 1-naphthyl group in **3c** was replaced with heterobicyclic rings. These efforts provided zoniporide (**3d**), which contains a 5-quinolinyl ring in place of the 1-naphthyl group. Zoniporide has excellent NHE-1 potency, which is 2- to 9-fold better than cariporide or eniporide, and an NHE-1 versus NHE-2 selectivity that is at least 3-fold higher. Furthermore, it has a rat NHE-3 IC_{50} >500,000 nM, which represents a >8000-fold selectivity against this isoform (Fig. 1). Interestingly, replacement of the cyclopropyl group of zoniporide with the methyl group present in the original lead structure results in a dramatic drop in NHE-1 potency and selectivity (compound **3e**). In fact, the combined effect of incorporating the cyclopropyl and 5-quinolinyl groups into this series appears to be synergistic. It is possible that steric interactions between the 5-quinolinyl ring and the cyclopropyl ring in zoniporide places both groups in an optimum conformation for both potency and selectivity.

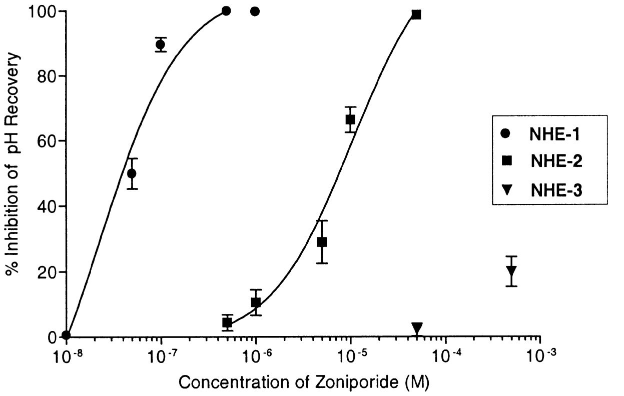

Figure 1. Zoniporide inhibition of human NHE-1-, NHE-2-, and rat NHE-3-mediated pH recovery in vitro using a FLIPR based assay. Values are means ± SE of representative data.

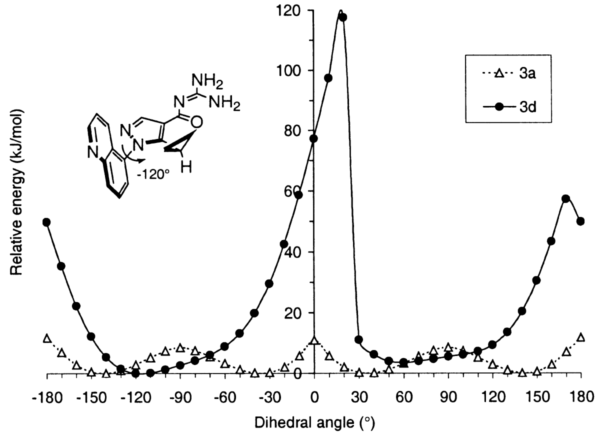

Figure 2. Rotational profile of **3a** about the phenyl-pyrazole bond, and of zoniporide (**3d**) about the quinoline-pyrazole bond. The structure shown represents the lowest energy conformer obtained for **3d**.

Computational molecular modeling[11] supports this hypothesis. Modeling of **3a** shows that the bond connecting the phenyl and pyrazole rings in this compound is conformationally flexible. As shown in Figure 2, even the highest energy rotamers around this bond are readily accessible (8–10 kJ/mol) and no particular conformation is favored (conformational dilution). Modeling of zoniporide (**3d**) provides very different results for the rotamers about the bond joining the quinoline and pyrazole rings (Fig. 2). An energy minimum is obtained at about −120°, and a valley with relative energy of 4 kJ/mol is observed at approximately 60°. The barriers to rotation of this bond are quite high: approximately 120 and 60 kJ/mol (at dihedral angles of about 20 and 170°, respectively). Thus, zoniporide appears to be considerably more conformationally rigid than **3a**.

The good aqueous solubility of zoniporide makes it well suited for a clinical target of parenteral administration. Crystalline zoniporide·$HCl·H_2O$ displays high solubility in several vehicles. For example, it has a solubility at room temperature of 5.6 and 8.4 mg of active/mL in sterile water for injection and 5% dextrose for injection, respectively. This is at least partially due to the presence of two distinct ionizable sites in the molecule. The pK_a of the acylguanidine and of the quinolinyl moieties are 7.2 and 3.4, respectively.

The pharmacology of zoniporide is very promising. A ^{22}Na uptake assay confirmed the high in vitro potency ($IC_{50} = 14$ nM) and selectivity (157-fold and 15,700-fold vs human NHE-2 and rat NHE-3, respectively) of zoniporide.[12] Its high selectivity for NHE-1 versus NHE-2 and NHE-3 diminishes the likelihood of side

Table 2. Pharmacokinetic parameters of zoniporide after intravenous administration in rat and dog[a]

Species	C_0[b] (μg/mL)	$AUC_{0-\infty}$ (μg·h/mL)	Clp (mL/min/kg)	Vdss (L/kg)	$t_{1/2}$ (h)	Plasma protein binding (%)
Rat ($n=4$)	0.28 (0.08)	0.07 (0.01)	237 (28)	7.2 (2.2)	0.5 (0.1)	54
Dog ($n=4$)	0.58 (0.08)	0.45 (0.15)	40 (13)	2.3 (0.2)	0.9 (0.3)	55

[a] Values are expressed as mean (standard deviation). Dose 1 mg/kg. All studies used zoniporide·$HCl·H_2O$ administered as a solution in normal saline.

[b] Represents the estimated plasma concentration at time zero calculated using log-linear back-extrapolation of the first two measured plasma concentrations.

effects due to interactions with the latter isoforms. Additionally, zoniporide displays excellent potency in an ex vivo inhibition of human platelet swelling assay ($IC_{50} = 54$ nM), which confirms its activity against endogenous human NHE-1.[12] Furthermore, zoniporide shows robust cardioprotection in the rabbit heart subjected to 30 min of regional ischemia and 2 h of reperfusion, both in vitro and in vivo ($EC_{50} = 0.25$ and 349 nM, respectively) with a maximum reduction of infarct size of 83 and 75%, respectively, in these models.[13]

Zoniporide displays the pharmacokinetics in rat and dog shown in Table 2, which should allow for intravenous administration. It is noteworthy that the plasma protein binding of zoniporide in these species is moderate. Renal clearance of unchanged drug is low in dogs (13%).

In conclusion, zoniporide is a potent and selective inhibitor of NHE-1, which exhibits high aqueous solubility and acceptable pharmacokinetics for intravenous administration. The potency and selectivity of zoniporide may be due to the conformation that the molecule adopts because of the presence of a cyclopropyl and a 5-quinolinyl substituent on the central pyrazole ring of the molecule. This compound may be useful in protecting the myocardium and other tissues from ischemia/reperfusion injury, and is currently the subject of further investigation.

Acknowledgements

The authors are grateful to Leanne M. Buzon, George C. Chang, Shane A. Eisenbeis, Melissa L. Gillaspy, Lisa M. Kath, Jaquelyn L. Klug, George Magnus-Aryitey and Michael R. Makowski for their synthetic contributions to the NHE-1 program. We thank Mark G. Biron, Eugene F. Fiese and Joseph E. Mertz for their pharmaceutical sciences input. The biology advice of Michael L. Mangiapane is gratefully acknowledged.

References and notes

1. (a) For recent reviews on the structure, function, regulation, isoforms and distribution of NHE, see: Counillon, L.; Pouyssegur, J. *J. Biol. Chem.* **2000**, *275*, 1. (b) Fliegel, L. *J. Thromb. Thrombolyis* **1999**, *8*, 9. (c) Avkiran, M.; Snabaitis, A. K. *J. Thromb. Thrombolyis* **1999**, *8*, 25. (d) Aharonovitz, O.; Grinstein, S. *Drug News Perspect.* **1999**, *12*, 105. (e) Counillion, L.; Touret, N.; Godart, H.; Pouysségur, J.Eur. Heart J. Suppl. **1999**, *1*, K2. (f) Harris, C.; Fliegel, L. *Int. J. Mol. Med.* **1999**, *3*, 315. (g) Diprov, P.; Fliegel, L. *FEBS Lett.* **1998**, *424*, 1. (h) Fliegel, L.; Murtazina, R.; Dibrov, P.; Harris, C.; Moor, A.; Fernandez-Rachubinski, F. A. *Biochem. Cell Biol.* **1998**, *76*, 735. (i) Kinsella, J. L.; Heller, P.; Froehlich, J. P. *Biochem. Cell Biol.* **1998**, *76*, 743. (j) Wakabayashi, S.; Shigekawa, M.; Pouyssegur, J. *Physiol. Rev.* **1997**, *77*, 51. (k) Orlowski, J.; Grinstein, S. *J. Biol. Chem.* **1997**, *272*, 22373.

2. For recent reviews on the role of NHE-1 in ischemia/reperfusion injury, see: (a) Karmazyn, M.; Gan, X. T.; Humphreys, R. A.; Yoshida, H.; Kusumoto, K. *Circ. Res.* **1999**, *85*, 777. (b) Orlowski, J. *Ann. N.Y. Acad. Sci.* **1999**, *874*, 346. (c) Karmazyn, M. *Ann. N.Y. Acad. Sci.* **1999**, *874*, 326. (d) Gumina, R. J.; Gross, G. J. *J. Thromb. Thrombolyis* **1999**, *8*, 39. (e) Karmazyn, M. *J. Thromb. Thrombolyis* **1999**, *8*, 33. (f) Myers, M. L. *J. Thromb. Thrombolyis* **1999**, *8*, 53. (g) Erhardt, L. R. W. *Am. J. Cardiol.* **1999**, *83*, 23G. (h) Buerke, M.; Rupprecht, H.-J.; von Dahl, J.; Terres, W.; Seyfarth, M.; Schultheiss, H.-P.; Richardt, G.; Sheehan, F. H.; Drexler, H. *Am. J. Cardiol.* **1999**, *83*, 19G. (i) Avkiran, M. *Am. J. Cardiol.* **1999**, *83*, 10G. (j) Avkiran, M. *Eur. Heart J. Suppl.* **1999**, *1*, K11. (k) Murphy, E.; Cross, H. R.; Steenbergen, C. *Eur. Heart J. Suppl.* **1999**, *1*, K18. (l) Hashimoto, K.; Sugiyama, A.; Xue, Y. X.; Aye, N. N.; Yamada, C.; Chino, D. *Eur. Heart J. Suppl.* **1999**, *1*, K31. (m) Karmazyn, M. *Eur. Heart J. Suppl.* **1999**, *1*, K38. (n) Levitsky, J.; Gurell, D.; Frishman, W. H. *J. Clin. Pharmacol.* **1998**, *38*, 887. (o) Karmazyn, M. *Keio J. Med.* **1998**, *47*, 65. (p) Karmazyn, M. *Cur. Res. Ion Channel Modulat.* **1997**, *3*, 3. (q) Fröhlich, O.; Karmazyn, M. *Cardiovasc. Res.* **1997**, *36*, 138.

3. For a recent review on NHE inhibitors, see: Kleemann, H. W.; Weichert, A. G. *IDrugs* **1999**, *2*, 1009.

4. (a) Weichert, A.; Faber, S.; Jansen, H. W.; Scholz, W.; Lang, H. J. *Arzneim.-Forsch.* **1997**, *47*, 1204. (b) Graul, A.; Prous, J.; Castañer, J. *Drugs Future* **1997**, *22*, 1197. (c) Graul, A.; Prous, J.; Castañer, J. *Drugs Future* **1998**, *23*, 1235. (d) Dhein, S.; Salameh, A. *Cardiovasc. Drug Rev.* **1999**, *17*, 134. (e) Scholz, W. *Eur. Heart J. Suppl.* **1999**, *1*, K45. (f) Karmazyn, M. *Expert Opin. Invest. Drugs* **2000**, *9*, 1099.

5. Baumgarth, M.; Beier, N.; Gericke, R. *J. Med. Chem.* **1997**, *40*, 2017.

6. Taylor, E. C.; Turchi, I. J. *Org. Prep. Proced. Int.* **1978**, *10*, 221.

7. Menozzi, G.; Mosti, L.; Schenone, P. *J. Heterocycl. Chem.* **1987**, *24*, 1669.

8. Ferlin, M. G.; Chiarelotto, G.; Basadonna, O.; Gia, O.; Mobolio, S.; Baccichetti, F.; Carlassare, F. *Farmaco* **1989**, *44*, 1141.

9. [1-(Quinolin-5-yl)-5-cyclopropyl-1*H*-pyrazole-4-carbonyl]-guanidine hydrochloride monohydrate (**3d**·HCl·H_2O): mp 154–156 °C; ^{1}H NMR (400 MHz, DMSO-d_6) δ 0.42 (m, 2H), 0.59–0.61 (m, 2H), 1.88–1.95 (m, 1H), 7.57 (dd, $J = 9$, 4 Hz, 1H), 7.67 (d, $J = 4$ Hz, 1H), 7.82 (d, $J = 7$ Hz, 1H), 7.90 (t, $J = 8$ Hz, 1H), 8.22 (d, $J = 8$ Hz, 1H), 8.38 (bs, 2H), 8.69 (bs, 2H), 8.72 (s, 1H), 8.98 (dd, $J = 4$, 1.4 Hz, 1H); ^{13}C NMR (100 MHz, DMSO-d_6) δ 7.8, 8.0, 114.8, 123.7, 125.3, 126.8, 129.6, 131.7, 131.8, 135.7, 141.6, 148.4, 151.2, 152.2, 156.3, 163.2; APCIMS 321 $[M+H]^+$. Anal. calcd for $C_{17}H_{16}N_6O{\cdot}HCl{\cdot}H_2O$: C, 54.47; H, 5.11; N, 22.42; Cl, 9.46. Found: C, 54.36; H, 5.16; N, 22.38; Cl, 9.13.

10. Materials: 2,7-Biscarboxyethyl-5,6-carboxyfluorescein acetoxymethyl (BCECF-AM) was purchased from Molecular Probes (Eugene, OR). All other reagents were of analytical grade and obtained commercially. Methods: PS120 fibroblast cells expressing human NHE-1 or rat NHE-3 isoforms were obtained from Professor J. Pouyssegur (Nice, France). Human NHE-2 expressing cells were generated at Pfizer Global Research and Development (Groton, CT). PS120 fibroblasts expressing indicated NHE isoform were grown to confluency in 96-well collagen coated plates. Measurement of intracellular pH (pH_i) was based on the methodology of: Russ, U.; Balser, C.; Scholz, W.; Albus, U.; Lang, H. J.; Weichert, A.; Scholkens, B. A.; Gogelein, H. *Pflugers Arch.* **1996**, *433*, 26. Cells were washed three times with assay buffer (10 mM Hepes, 136 mM NaCl, 5.4 mM KCl, 0.44 mM KH_2PO_4, 0.34 mM Na_2HPO_4, 1 mM $CaCl_2$, 1 mM $MgCl_2$ and 5.6 mM glucose, pH 7.4) followed by incubation with 5 μM BCECF-AM in the same buffer for 30 min at 37 °C. Cells were then washed seven times with acid loading buffer (30 mM NH_4Cl, 90 mM choline chloride, 5 mM KCl, 1.8 mM $CaCl_2$, 1 mM $MgCl_2$, 5 mM

glucose, and 15 mM Hepes, pH 7.5). Cells were initially incubated for 1 h with acid loading buffer followed by an additional 5 min incubation in the presence or absence of test compounds. Initial baseline fluorescence was recorded for each well simultaneously using a fluorescence-imaging plate reader (FLIPR). Intracellular acidification was induced by the addition of assay buffer with or without test compound. Intracellular acidification was observed as a marked reduction of BCECF fluorescence. NHE inhibitors prevent recovery from the acidification (measured as fluorescent units). Data analysis: The potency of NHE inhibitors was calculated as a function of its ability to prevent recovery from acidification compared with control. The IC_{50} value for NHE inhibitors (concentration required to inhibit pH_i recovery by 50%) was calculated by fitting the data via nonlinear least squares regression analysis to the equation: % Inhibition $= 100/[1+(10^C/10^X)^D]$, where $X = \log$ [drug concentration], C (IC_{50}) $= \log$ [drug concentration at 50% inhibition], and $D =$ the Hill coefficient.

11. Conformational analyses were performed using the OPLS/A force field with the GBSA solvent approximation as implemented in MacroModel v.7. Low energy conformers were identified via a Monte Carlo search, followed by energy minimization. Rotations were allowed for all single, acyclic and non-terminal bonds. All of the low energy conformers place the cyclopropyl group in the conformation with respect to the pyrazole ring shown in Figure 2. The rotational profiles in Figure 2 were generated using the low energy conformers identified in the Monte Carlo search as the initial structures. The bond of interest was held fixed at 10° increments and a constrained energy minimization was performed on each of these rotamers.

12. Marala, R. B.; Brown, J. A.; Kong, J. X.; Tracey, W. R.; Knight, D. R.; Wester, R. T.; Sun, D.; Kennedy, S. P.; Hamanaka, E. S.; Ruggeri R. B.; Hill, R. J., submitted for publication.

13. Knight, D. R.; Smith, A. H.; Flynn, D. M.; MacAndrew, J. T.; Ellery, S. S.; Kong, J. X.; Marala, R. B.; Wester, R. T.; Guzman-Perez, A.; Hill, R. J.; Magee, W. P.; Tracey, W. R. *J. Pharmacol. Exp. Ther.* **2001**, *297*, in press.